Journal Title
XX(X):1–31

DOI: 10.1177/ToBeAssigned
www.sagepub.com/
SAGE

An internal variable model of macroscopic twin boundary dynamics

Arkadi Berezovski

Abstract

Depending on whether the experiments are quasi-static or fast dynamics, the measured twin boundary velocity values range from zero to the material's sound speed. The twin boundary velocity is not yet predicted theoretically in the continuum mechanics framework. The extension of continual description is provided in the paper by means of internal variables. It is shown that a diffusional slow motion of twin boundaries can be represented using a single internal variable. The dual internal variable technique is employed for the description of the fast dynamics of twin boundaries.

Keywords

twin boundary dynamics,internal variables,macroscopic description

1 Introduction

Twins are planar defects of the crystal lattice that can be represented as coherent interfaces between identical but differently oriented lattices. One of the most essential features of twins is their ability to move in response to external forces, which results in growth of one of the differently oriented lattices and carries a macroscopic deformation of the material. Twin boundary motion is especially essential in shape memory alloys

Department of Cybernetics, School of Science, Tallinn University of Technology, Ehitajate tee 5, 19086 Tallinn, Estonia
Email: arkadi.berezovski@taltech.ee

(Otsuka and Wayman 1999; Bhattacharya 2003), where the twins appear between different variants of martensite. The reversible reorientation of martensite via twins motion is the key mechanism of pseudoplastic straining of shape memory alloys, and the speed of this process can be decisive for the overall mechanical performance of the alloy.

The study of mechanical twins has a long history (Duparc 2017). For a long time, it was considered that twins grew at exceptionally rapid rates due to audible sounds detected during the twinning process. (Mahajan and Williams 1973; Reed-Hill et al. 1973). The rapid growth of twins has been confirmed by experiments by Takeuchi (1966) who reported the value 2570 m/s for twin head velocity in iron single crystals, by Williams and Reid (1971) with 2250 m/s for the velocity of twin tip in silicon-iron alloy, and by recent in-situ high speed optical imaging of twin tip propagation in single crystal magnesium reaching 2000 m/s (Kannan et al. 2018).

Furthermore, the theoretical prediction by Rosakis and Tsai (1995) of possibly intersonic twin development was confirmed experimentally for ferroelectric crystals (Faran and Shilo 2010) and for single-crystal aluminum (Zhao et al. 2016).

Bowden and Cooper (1962) on the other hand, reported that the observed velocity of twin propagation in zinc crystals under explosive loading ranged from 30 m/s to 300 m/s. In situ measurements of twin boundary motion by Smith et al. (2014) in the magnetic shape memory alloy Ni–Mn–Ga gave a value of 82.5 m/s for the twin boundary velocity. The twin boundary velocity in Ni–Mn–Ga 5 M martensite recorded with a high-speed camera was determined to be 39 m/s (Saren et al. 2016).

However, this is not the smallest experimentally recorded value for the velocity of the twin boundary. According to Mizrahi et al. (2020), dynamic force pulse tests on a 10M Ni–Mn–Ga single crystal produced twin boundary velocity values ranging from 0 to 14 m/s. Furthermore, the twin boundary velocity in a slow rate experiment is typically 10^{-5} m/s, as mentioned in (Shilo et al. 2021).

The significant scatter in the experimental data requires a better understanding of the dynamics of twin boundaries. Various aspects of twin boundary motion have been studied theoretically and computationally. Phase field models (Hu et al. 2010; Levitas et al. 2013; Grilli et al. 2020; Amirian et al. 2022, c.f.), crystal plasticity model (Mirkhani and Joshi 2014, e.g.) and their combinations (Liu et al. 2018; Rezaee-Hajidehi et al. 2022) do not consider individual twin boundaries. Quasi-static micromechanics-based models (Faran and Shilo 2011, 2014; Danino et al. 2019; Shilo et al. 2021) are concentrated on their own experimental data. Fast moving twin boundaries (Seiner 2015; Seiner et al. 2022, e.g.) are beyond the scope of models by Faran and Shilo.

The common approach to the continuum description of twin boundaries, and phase fronts in diffusionless phase transitions in general, is to assume a multi-well energy landscape $W(u_x)$, where individual minima on the strain energy density represent the individual equilibrium states, or variants. This approach, however, requires either dealing with higher-order polynomials for the elastic energy (the Landau-energy landscape framework (Falk 1980; Rasmussen et al. 2001; Gu et al. 2013; Zoubková et al. 2022, c.f.)) or assuming the energy landscape as piece-wise quadratic with discontinuity in second derivatives (Abeyaratne and Knowles 2006). In both cases, issues about the nature and height of the barrier between the energy wells arise, and the velocity of phase boundaries cannot be predicted uniquely. As a result, the continuum description of twin boundary propagation is incomplete. The incompleteness is resolved using a special Landau functional structure (Shchyglo et al. 2012) or a kinetic relation (Abeyaratne and Knowles 2006). In both cases, additional constitutive assumptions are introduced.

A new approach is provided by the dual internal variable theory (Ván et al. 2008; Berezovski and Ván 2017; Berezovski 2018, 2023). This study reveals how to model both slow and fast twin boundary propagation in the continuum mechanics framework enhanced by dual internal variables. For simplicity, we focus on a uniaxial situation with a scalar transverse displacement field $u(x)$ where two lattices distinguished by one-dimensional shear strains $u_x = \pm\varepsilon^{tr}/2$. We will hereafter refer to these two lattices as to twins.

1.1 Uniaxial twin boundary motion

Uniaxial motion implies that all fields are dependent on a single coordinate and time. Longitudinal and transverse motions are uncoupled in the uniaxial setting. We disregard longitudinal motion by focusing on shear strains. Restricting by the transverse displacement u

$$u = u(x,t), \tag{1}$$

we apply the balance of linear momentum in the isothermal case (without body forces) as

$$\rho v_t = \sigma_x. \tag{2}$$

Here σ is the shear stress, $v = u_t$ is the transverse particle velocity, ρ is the constant matter density, and subscripts denote derivatives. The kinematic compatibility condition reads

$$\varepsilon_t = v_x, \tag{3}$$

where $\varepsilon = u_x$ is the shear strain.

1.2 Jump conditions

Let the possibly moving twin boundary $\mathcal{S}$ splitting the variants be located at a certain position x_0. The following jump relation is satisfied at this boundary in the context of the continuum description (Abeyaratne and Knowles 2006, e.g.):

$$V_N \left[\!\left[\rho v\right]\!\right] + \left[\!\left[\sigma\right]\!\right] = 0, \tag{4}$$

Here V_N is the velocity of the moving twin boundary, and $\left[\!\left[B\right]\!\right] = B^+ - B^-$, $B^\pm$ are uniform limits of a field B in approaching the boundary from its positive and negative sides, respectively.

The driving force $f_\mathcal{S}$ acting on the boundary is determined by (Abeyaratne and Knowles 2006)

$$f_\mathcal{S} = \left[\!\left[W\right]\!\right] - \langle\sigma\rangle \left[\!\left[\varepsilon\right]\!\right], \tag{5}$$

where W is the free energy per unit volume and $\langle ...\rangle$ denotes the arithmetical mean.

1.3 Twin boundary velocity

The velocity of the twin boundary is determined by the relationship

$$\rho V_N^2 \left[\!\left[\varepsilon\right]\!\right] = \left[\!\left[\sigma\right]\!\right], \tag{6}$$

which follows from jump relation (4) and that for the jump of the kinematic compatibility condition (3)

$$\left[\!\left[v\right]\!\right] = - \left[\!\left[\varepsilon\right]\!\right] V_N. \tag{7}$$

The sign of the velocity of the twin boundary follows from the entropy inequality on the twin boundary (Abeyaratne and Knowles 2006)

$$f_\mathcal{S} V_N \geq 0. \tag{8}$$

It should be noted that the lack of uniqueness exists for the relevant initial-boundary value problem (Abeyaratne and Knowles 1990) since the stress jump in Eq. (6) is not known in advance.

1.4 Isothermal twins equilibrium

We consider a material with two possible twin variants. We assume that the variants are energetically equivalent, which means that material points in both variants have the same energy value. It is also assumed that the elastic parameters for both variants are the same. In uniaxial setting, the elastic free energy per unit volume is the quadratic function of shear strain

$$W = \frac{G}{2} u_x^2. \tag{9}$$

Here G is the shear modulus of the material and subscript denotes the space derivative. It is obvious that the energy value is the same for $+u_x$ and $-u_x$.

Assume the variants occupy adjacent parts of a body separated by a twin boundary. We will investigate the conditions for the coexistence of the variants in equilibrium state. Although the equilibrium state implies that there is no motion ($u = 0$), shear strains can have non-zero values in both variants. Positive strains are associated with variant 1 and negative strains with variant 2. It is well known that the strains in distinct twins differ from one another by the so-called transformation strain ε^{tr}. Because of the symmetry, the shear strain values can be specified as follows:

$$\varepsilon_1 = \frac{1}{2}\varepsilon^{tr}, \quad \varepsilon_2 = -\frac{1}{2}\varepsilon^{tr}. \tag{10}$$

This keeps the equality of the free energy in both variants. Here lower indices indicate twin variants.

It is reasonable to assume that in equilibrium the value of stress is equal to zero. However, the stress is linear in strain

$$\sigma = \frac{\partial W}{\partial \varepsilon} = G\varepsilon, \tag{11}$$

which leads to the following values of the stress in distinct variants:

$$\sigma_1 = G\varepsilon_1 = \frac{G}{2}\varepsilon^{tr}, \quad \sigma_2 = G\varepsilon_2 = -\frac{G}{2}\varepsilon^{tr}. \tag{12}$$

It follows that the stress equality cannot be achieved in the macroscopic representation.

As a result, the macroscopic exposition encounters problems with both equilibria of twins and twin boundary motion. It is clear that the continuum description of twin boundary dynamics should be expanded. We will employ internal variables to increase the degree of freedom in the representation.

1.5 Internal variables

The idea of the use of internal variables is not new. It has been exploited intensively in the modeling of shape memory alloys (Tanaka and Nagaki 1982; Tanaka et al. 1986; Brinson 1993; Brinson and Huang 1996; Auricchio and Lubliner 1997). As a rule, individual phase boundaries were not considered because the internal variable was the martensitic volume fraction with a prescribed transformation kinetics (Sadjadpour and Bhattacharya 2007; Mirzaeifar et al. 2011; Song 2020). Variants of transformation kinetics have been reviewed in (Paiva and Savi 2006; Khandelwal and Buravalla 2009).

This paper employs another internal variable approach (Berezovski and Ván 2017; Berezovski 2018, 2023). Here internal variables characterize the difference between twins. This makes it possible to use them to identify twin boundaries. Basic notions of this internal variables method are presented in Appendix.

Internal variables allow us to avoid non-convexity and/or non-smoothness in the energy density function $W(u_x)$ by introducing extra degrees of freedom. We start with a single internal variable case. Here we assume that the elastic response of each twin variant is governed by a quadratic energy well with a switching parameter that specifies in which variant the material is. This parameter is the gradient of the internal variable. The free energy per unit volume is then represented as

$$W(u_x, \varphi_x) = \frac{G}{2}u_x^2 + \frac{1}{2}Au_x\varphi_x + \frac{1}{2}C\varphi_x^2, \tag{13}$$

where A and C are constants, and φ is the internal variable. For setting $A = G\varepsilon^{tr}$, the stress is determined in the form

$$\sigma = \frac{\partial W}{\partial u_x} = G\left(u_x + \frac{1}{2}\varepsilon^{tr}\varphi_x\right), \tag{14}$$

which enables switching between two stress-free states with $u_x = \varepsilon^{tr}/2$ and $u_x = -\varepsilon^{tr}/2$, respectively, by setting the parameter φ_x equal to -1 and 1. These two states represent the two energy minima associated with two twin variants In Section 3, we will demonstrate that this formalism can capture the slow-dynamics response of the system to quasi-static loading.

For fast dynamics, where the inertia of the material is essential, we show that the propagation of a twin boundary can be described using a dual variable model (Section 4), assuming the energy density function of form

$$W(u_x, \varphi_x, \psi) = \frac{G}{2}u_x^2 + \frac{1}{2}Au_x\varphi_x - \frac{1}{2}C\varphi_x^2 - \frac{1}{2}D\psi^2, \tag{15}$$

where the last term with the dual internal variable ψ ensures that the evolution equations for the internal variables are in this case hyperbolic, as elaborated in detail in Appendix. As a result, wave-like propagating solutions for the switching parameter φ_x allow fast-moving, inertia-driven twin boundaries.

2 Single internal variable

In the single internal variable case, the free energy W per unit volume is specified as a quadratic function of the shear strain, the internal variable, φ, and its space gradient φ_x (Maugin and Muschik 1994, e.g.)

$$W = \frac{G}{2}u_x^2 + \frac{1}{2}Au_x\varphi_x + \frac{1}{2}C\varphi_x^2, \tag{16}$$

with material parameters $A = G\varepsilon^{tr}$ and C. We consider here a reduced version of the free energy dependence because only the gradient of internal variable is included.

To distinguish twin variants, we suppose that internal variable gradients have alternating signs. If for the variant 1 we assume the negative sign of the gradient of internal variable, then for variant 2 it should be positive.

By definition, the shear stress is calculated as

$$\sigma = \frac{\partial W}{\partial u_x} = G\left(u_x + \frac{1}{2}\varepsilon^{tr}\varphi_x\right). \tag{17}$$

If $\varphi_x = -1$ then the value of the shear stress

$$\sigma_1 = G\left((u_x)_1 - \frac{1}{2}\varepsilon^{tr}\right), \tag{18}$$

corresponds to variant 1. For variant 2 we have, accordingly, $\varphi_x = 1$ and

$$\sigma_2 = G\left((u_x)_2 + \frac{1}{2}\varepsilon^{tr}\right). \tag{19}$$

2.1 Equilibrium conditions

To be more specific, let us consider the uniaxial state of a bar which may contain two kinds of twin variants. The bar occupies the region $0 < x < L$. Suppose that variant 1 occupies the part of the bar $0 < x < l_1$ and variant 2 is in the rest of the bar. The state of each twin variant is determined by the values of shear strains ε_1 and ε_2 and gradients of internal variable $(\varphi_1)_x = \gamma_1$ and $(\varphi_2)_x = \gamma_2$. It is reasonable to assume that both twins are stress-free in equilibrium. The following shear strain values relate

to zero stress levels:

$$\varepsilon_1 = \frac{1}{2}\varepsilon^{tr}, \quad \varepsilon_2 = -\frac{1}{2}\varepsilon^{tr}. \tag{20}$$

Accordingly, the driving force acting at the twin boundary reduces to the jump of the free energy in the stress-free equilibrium

$$f_{\mathcal{S}} = [\![W]\!] - \langle\sigma\rangle [\![\varepsilon]\!] = [\![W]\!]. \tag{21}$$

Calculating the free energy jump

$$\begin{aligned}
&(W_2 - W_1) = \left(\frac{G}{2}\varepsilon_2^2 + \frac{1}{2}A\varepsilon_2\gamma_2 + \frac{1}{2}C\gamma_2^2\right) - \\
&- \left(\frac{G}{2}\varepsilon_1^2 + \frac{1}{2}A\varepsilon_1\gamma_1 + \frac{1}{2}C\gamma_1^2\right) = \\
&= \frac{G}{2}\left(\varepsilon_2^2 - \varepsilon_1^2\right) + \frac{1}{2}G\varepsilon^{tr}\left(\varepsilon_2\gamma_2 - \varepsilon_1\gamma_1\right) + \frac{1}{2}C\left(\gamma_2^2 - \gamma_1^2\right) + \sigma_0\varepsilon^{tr} = \\
&= \frac{G}{2}(\varepsilon_2 - \varepsilon_1)(\varepsilon_2 + \varepsilon_1) + \frac{1}{2}G\varepsilon^{tr}\left(\varepsilon_2\gamma_2 - \varepsilon_1\gamma_1\right) + \\
&+ \frac{C}{2}(\gamma_2 - \gamma_1)(\gamma_2 + \gamma_1) = 0,
\end{aligned} \tag{22}$$

we obtain zero value because of conditions $\varepsilon_1 + \varepsilon_2 = 0$ and $\gamma_2 + \gamma_1 = 0$. As a result, there is no driving force at the twin boundary in equilibrium, as expected. Thus, the introduction of the internal variable enables the twins to achieve a stress-free equilibrium. The obtained relationships serve as initial conditions for a possible motion of the twin boundary.

3 Slow motion

To determine a possible motion of the twin boundary, we need to calculate the value of the driving force in non-equilibrium situation

$$
\begin{aligned}
f_{\mathcal{S}} = [\![W]\!] - \langle\sigma\rangle [\![\varepsilon]\!] = \left(\frac{G}{2}\varepsilon_2^2 + \frac{1}{2}A\varepsilon_2\gamma_2 + \frac{1}{2}C\gamma_2^2\right) - \\
- \left(\frac{G}{2}\varepsilon_1^2 + \frac{1}{2}A\varepsilon_1\gamma_1 - \frac{1}{2}C\gamma_1^2\right) - \frac{1}{2}(\sigma_2+\sigma_1)(\varepsilon_2-\varepsilon_1) = \\
= \frac{G}{2}\left(\varepsilon_2^2 - \varepsilon_1^2\right) + \frac{1}{2}G\varepsilon^{tr}\left(\varepsilon_2\gamma_2 - \varepsilon_1\gamma_1\right) + \frac{1}{2}C\left(\gamma_2^2 - \gamma_1^2\right) + \\
+ \frac{1}{2}\left(G(\varepsilon_2 + \frac{1}{2}\varepsilon^{tr}\gamma_2) + G(\varepsilon_1 + \frac{1}{2}\varepsilon^{tr}\gamma_1)\right)(\varepsilon_2-\varepsilon_1) = \\
= \frac{1}{2}G\varepsilon^{tr}\left(\varepsilon_2\gamma_2 - \varepsilon_1\gamma_1\right) + \frac{1}{2}C\left(\gamma_2^2 - \gamma_1^2\right) + \frac{1}{2}G\varepsilon^{tr}\langle\gamma\rangle(\varepsilon_2-\varepsilon_1),
\end{aligned}
\tag{23}
$$

which is non-zero anymore. The twin boundary velocity is then determined as

$$
V_N^2 = \frac{[\![\sigma]\!]}{\rho\,[\![\varepsilon]\!]} = \frac{G(\varepsilon_2 + \frac{1}{2}\varepsilon^{tr}\gamma_2) - G(\varepsilon_1 + \frac{1}{2}\varepsilon^{tr}\gamma_1)}{\rho\,[\![\varepsilon]\!]} = \frac{G}{\rho}\left(1 + \frac{\varepsilon^{tr}}{[\![\varepsilon]\!]}\frac{\gamma_2-\gamma_1}{2}\right). \tag{24}
$$

If the value of the driving force exceeds a certain threshold, the boundary between the twins is expected to shift. The change of twins state is governed by the dimensionless balance of linear momentum

$$
\bar{v}_t = \bar{\varepsilon}_x + \frac{A}{2G}\bar{\gamma}_x, \tag{25}
$$

and the evolution equation for the internal variable

$$
\bar{\gamma}_t = \frac{C}{A}\bar{\gamma}_{xx} + \frac{1}{2}\bar{\varepsilon}_{xx}. \tag{26}
$$

Details of the derivation of the evolution equation for the gradient of the internal variable are given in Appendix. The gradient of the internal variable can be interpreted as an order parameter because its evolution equation is of the Ginzburg-Landau type. It should be noted that Eqs. (25) and (26) are coupled and non-reflecting boundary conditions are applied at ends of the bar.

3.1 Numerical example

For numerical test, the length of the bar is divided by 1000 space steps. The boundary between twins is placed at the point corresponding to 400 space steps. The left part of the specimen is occupied by the variant 1 (marked by yellow color in Fig. 1).

Figure 1. Sketch of initial twins position.

The values of shear strains in twins are chosen as follows:

$$\varepsilon_1 = 0.02, \quad \varepsilon_2 = -0.02, \quad \varepsilon^{tr} = 0.04. \tag{27}$$

Gradients of the internal variable follow conditions

$$\gamma_1 = -1, \quad \gamma_2 = 1. \tag{28}$$

The choice of the parameters corresponds to an equilibrium state with zero shear stress value. Initial distributions of shear strains and gradients of the internal variable are illustrated in Figs. 2 and 3.

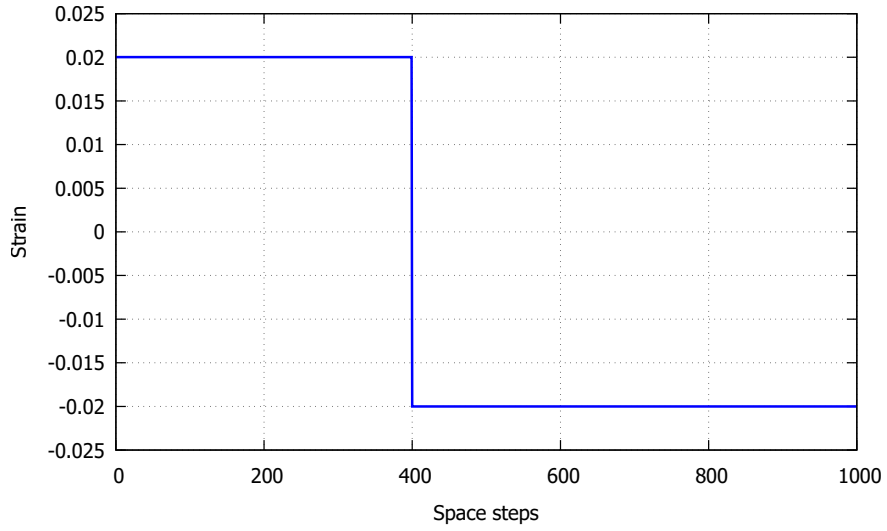

Figure 2. Equilibrium shear strain distribution.

It is clear that the equilibrium state will not change in the absence of external influence. Consider now the situation where the variant 1 (as a whole) receives an additional amount of energy from external sources. The time history of the loading is shown at Fig. 4. Suppose that this additional energy leads to the value of the driving

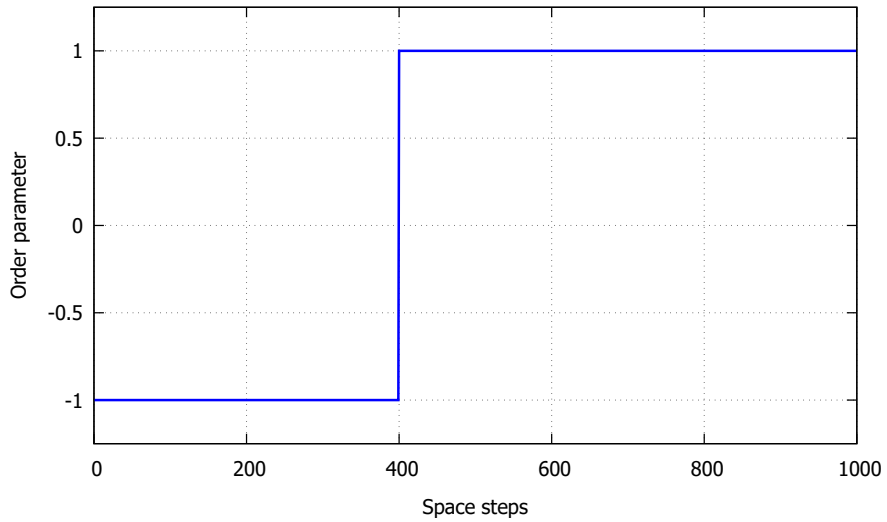

Figure 3. Equilibrium distribution of the gradient of the internal variable γ.

force above the critical value. The placement of the boundary between variants will change accordingly.

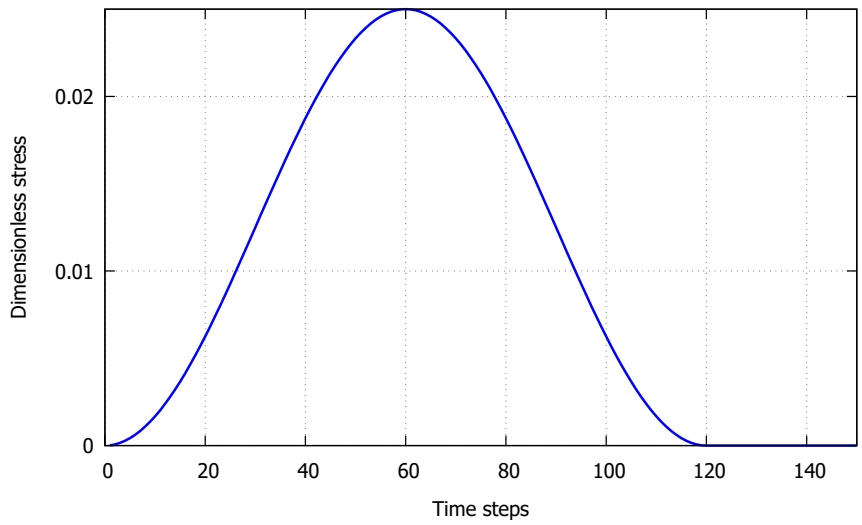

Figure 4. Shear stress variation in time in the variant 1.

The twin boundary motion is simulated numerically. Starting with the initial equilibrium state shown in Figs. 2 and 3, new shear strains and gradients of the internal variable are computed in each time step solving Eqs. (25) and (26). Computations are performed by the thermodynamically consistent finite volume numerical scheme (Berezovski et al. 2008). The main feature of the used scheme is the ability to determine the value of the stress jump at the moving boundary algorithmically (Berezovski et al. 2008). This eliminates the non-uniqueness in the solution. The corresponding driving force and a possible velocity of the twin boundary are calculated following Eqs. (23) and (24). The motion of the twin boundary is allowed only if the value of the driving force overcomes a critical value.

The twin boundary motion is manifested by the change in the distributions of shear strain and gradient of the internal variable at different time instants as shown in Figs. 5 and 6. The distribution of the shear strain is plotted sequentially for every 50 time steps in Fig. 5, beginning with that for 50 time steps. The shifted shape of the shear strain distribution is clearly visible. The upper line represents the new equilibrium state.

A similar plot for the distribution of the gradient of the internal variable is displayed in Fig. 6. It is noteworthy that the gradient of the internal variable exhibits typical order parameter behavior.

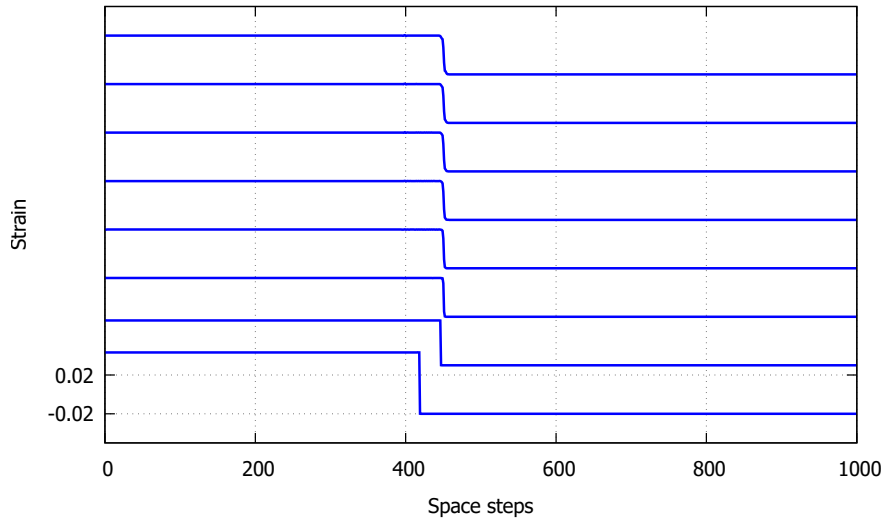

Figure 5. Shift of the shear strain distribution over time.

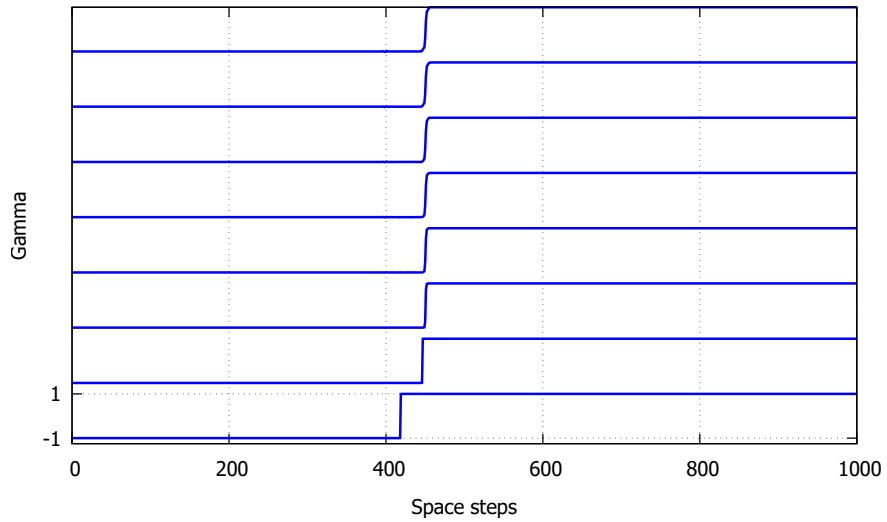

Figure 6. Change in the distribution of the gradient of the internal variable over time.

The results of the calculation of the variation of the position of the twin boundary over time are shown in Fig. 7. The position of the twin boundary changes nonlinearly in response to the external load from its initial value (400 space steps) to a final one. It corresponds to the shift in shear strain and gradient of internal variable presented in Figs. 5 and 6. After the external loading is reduced, the twin boundary stops moving.

The dependence of the velocity of the twin boundary on the driving force is presented in Fig. 8. It represents a typical kinetic relation curve.

3.2 Asymptotics of the strain jump

For a small deviation of the actual shear strain jump from the value of the transformation strain, we can represent the shear strain jump as an asymptotic expansion

$$[\![\varepsilon]\!] = \varepsilon^{tr}(1 + \delta\epsilon^1 + \ldots), \tag{29}$$

with a small parameter δ.

In such a case, the velocity of the twin boundary is, in the first approximation,

$$V_N^2 = \frac{G}{\rho}\left(1 + \frac{\varepsilon^{tr}}{[\![\varepsilon]\!]}\frac{\gamma_2 - \gamma_1}{2}\right) \approx \frac{G}{\rho}\delta\epsilon^1, \tag{30}$$

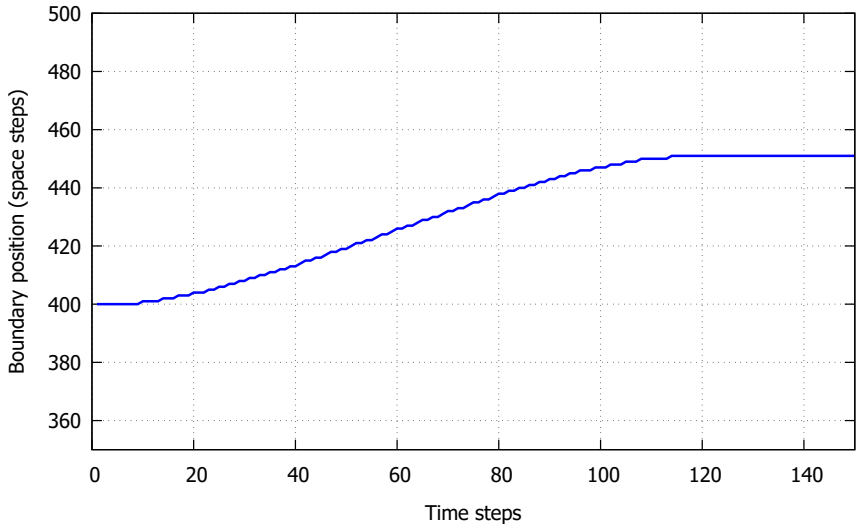

Figure 7. Variation of the position of the twin boundary in time.

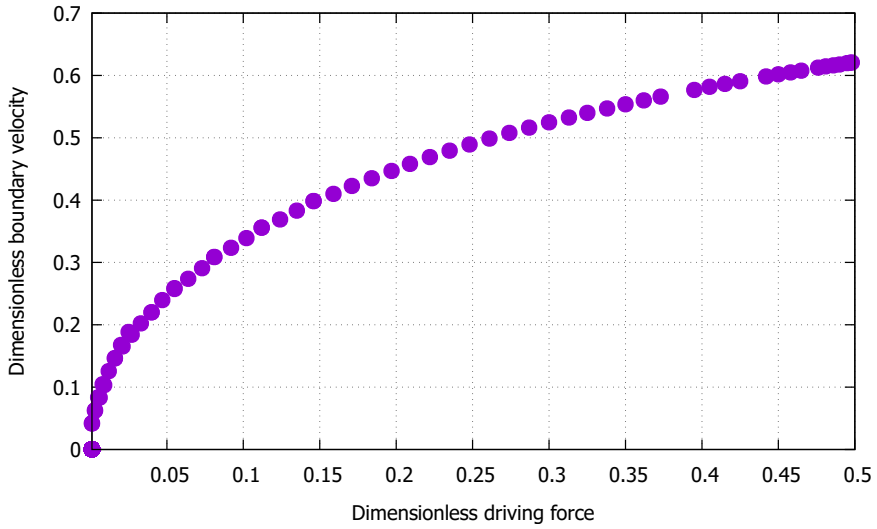

Figure 8. Boundary velocity vs driving force.

because the value of $\gamma_2 - \gamma_1$ is close to 2 in the vicinity of twin boundary. It is clear that the value of the twin boundary velocity can be as small as that dictated by the value of δ in a particular situation. The slow motion of the twin boundary corresponding to the

single internal variable model correlates to results of quasi-static experiments (Faran and Shilo 2011, 2016; Mizrahi et al. 2020; Shilo et al. 2021). However, the single internal variable model is insufficient for fast dynamics of twin boundaries because it exploits a parabolic evolution equation for the internal variable.

4 Fast dynamics

4.1 Dual internal variables

We apply the dual internal variable approach (Berezovski and Ván 2017; Berezovski 2018) to go beyond the diffusional description. The complete theory of dual internal variables is presented in (Berezovski and Ván 2017). Here we use a reduced version of the theory assuming that the free energy density depends on internal variables φ and ψ by virtue of a quadratic function

$$W = \frac{G}{2}u_x^2 + \frac{1}{2}A\varphi_x u_x - \frac{1}{2}C\varphi_x^2 - \frac{1}{2}D\psi^2, \tag{31}$$

where material parameters $A = G\varepsilon^{tr}$, C, and D are constant. In this version, the free energy does not depend on the internal variable φ explicitly and on the gradient of the internal variable ψ. Negative signs for coefficients C and D are applied in the correspondence to (Berezovski 2016).

Shear stress values are calculated as previously

$$\sigma = \frac{\partial W}{\partial u_x} = G\left(u_x + \frac{1}{2}\varepsilon^{tr}\varphi_x\right). \tag{32}$$

4.2 Driving force and twin boundary velocity

In the case of dual internal variables, the expression for the driving force takes the form

$$\begin{aligned} f_{\mathcal{S}} = [\![W]\!] - \langle\sigma\rangle [\![\varepsilon]\!] &= \left(\frac{G}{2}\varepsilon_2^2 + \frac{1}{2}A\varepsilon_2\gamma_2 - \frac{1}{2}C\gamma_2^2 - \frac{1}{2}D\psi_2^2\right) - \\ &- \left(\frac{G}{2}\varepsilon_1^2 + \frac{1}{2}A\varepsilon_1\gamma_1 - \frac{1}{2}C\gamma_1^2 - \frac{1}{2}D\psi_1^2\right) - \frac{1}{2}(\sigma_2+\sigma_1)(\varepsilon_2-\varepsilon_1) = \\ &= \frac{G}{2}\left(\varepsilon_2^2 - \varepsilon_1^2\right) + \frac{1}{2}G\varepsilon^{tr}\left(\varepsilon_2\gamma_2 - \varepsilon_1\gamma_1\right) - \frac{1}{2}C\left(\gamma_2^2 - \gamma_1^2\right) - \\ &- \frac{1}{2}D\left(\psi_2^2 - \psi_1^2\right) - \frac{1}{2}\left(G(\varepsilon_2 + \frac{1}{2}\varepsilon^{tr}\gamma_2) + G(\varepsilon_1 + \frac{1}{2}\varepsilon^{tr}\gamma_1)\right)(\varepsilon_2 - \varepsilon_1) = \\ &= \frac{1}{2}G\varepsilon^{tr}\left(\varepsilon_2\gamma_2 - \varepsilon_1\gamma_1\right) - C[\![\gamma]\!]\langle\gamma\rangle - D[\![\psi]\!]\langle\psi\rangle - \frac{1}{2}G\varepsilon^{tr}\langle\gamma\rangle[\![\varepsilon]\!]. \end{aligned} \tag{33}$$

The value of the twin boundary velocity is calculated accordingly

$$V_N^2 = \frac{[\![\sigma]\!]}{\rho\,[\![\varepsilon]\!]} = \frac{G(\varepsilon_2 + \frac{1}{2}\varepsilon^{tr}\gamma_2) - G(\varepsilon_1 + \frac{1}{2}\varepsilon^{tr}\gamma_1)}{\rho\,[\![\varepsilon]\!]} = \frac{G}{\rho}\left(1 + \frac{\varepsilon^{tr}(\gamma_2 - \gamma_1)}{2\,[\![\varepsilon]\!]}\right). \tag{34}$$

As shown in Appendix, the dual internal variable ψ is proportional to the time rate of the primary internal variable φ

$$\psi = \frac{1}{D}\varphi_t. \tag{35}$$

4.3 Governing equations

The main difference between single and dual internal variables approaches is that the evolution equation for the internal variable φ in the dual internal variable theory is hyperbolic. The dimensionless form of the evolution equation is (see Appendix)

$$\frac{I}{\rho}\Phi_{tt} = \frac{C}{G}\Phi_{xx} - \frac{A}{2G}U_{xx}, \tag{36}$$

with $I = 1/D$.

The dimensionless balance of linear momentum (2) takes the form

$$U_{tt} = U_{xx} + \frac{A}{2G}\Phi_{xx}. \tag{37}$$

Dimensionless governing parameters of the problem are I/ρ, A/G, and C/G. These parameters can be chosen in such a way that the hyperbolicity of the equation of motion will be kept. In the simplest choice the value of I/ρ can be equal to unity. Remaining parameters depend on the transformation strain as in the case of the single internal variable. Just this values of governing parameters are used in the test problem below.

To determine the state of twins at each time step, system of coupled hyperbolic equations (36) and (37) is solved by means of the finite volume numerical scheme described in detail in (Berezovski et al. 2008).

4.4 Numerical example

Simulating the fast dynamics of a twin boundary, we deal with non-equilibrium states. Here the entire bar is assumed to be in variant 2 characterizing by $\varepsilon = -0.02$ for zero stress condition. The bar is elastically loaded in shear such that the resulting value of $\varepsilon_2 = 0.01$. This corresponds to the value of the dimensionless initial shear stress $\sigma_2 = 0.03$. The value of the gradient of the internal variable γ_2 is equal to 1.

Now we consider a setting in which a nucleus of variant 1 is suddenly formed in the middle of the bar. Initially, the shear strain in the nucleus is the same as in the variant 2, i.e., $\varepsilon_1 = 0.01$. This value of the shear strain corresponds to the stress value $\sigma_1 = -0.01$. The variant 1 is characterized by the value of the gradient of the internal variable $\gamma_1 = -1$. The size of the nucleus is taken as 20 space steps. The jumps in values of stress and the gradient of the internal variable γ induce a motion of the twin boundary. Additionally, we prescribe the time rate of the internal variable φ_t, which is connected to the dual internal variable ψ by Eq. (35). Its value is chosen as zero for the variant 2. Since there is no tools for the determination of the value of the time rate of the internal variable in advance, it is chosen from simulations. The best results are obtained for the value $(\varphi_t)_1 = 2$.

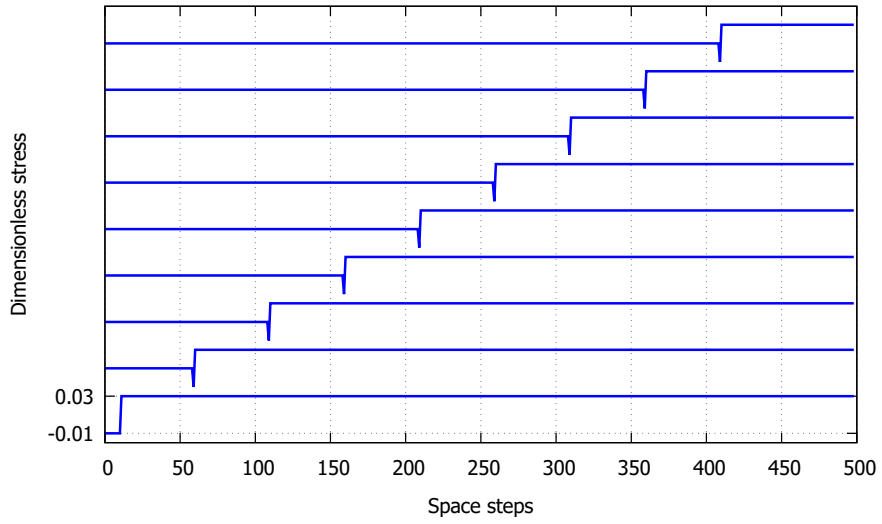

Figure 9. Distribution of shear stress along the bar plotted sequentially for every 50 time steps beginning with that for 50 time steps. The lowest line corresponds to the initial situation.

Numerical solution of governing equations (36)–(37) under implemented conditions results in the fast grow of the area of variant 1. It appears that the stress jump at the moving twin boundary is conserved after the adaptation of its value forced by the initial jump (Fig. 9). Due to the symmetry of the problem, only right half of the bar is shown.

The corresponding evolution of the shear strain distribution in time is presented in Fig. 10. It is seen clearly how the variant 1 consecutively occupies the bar that was

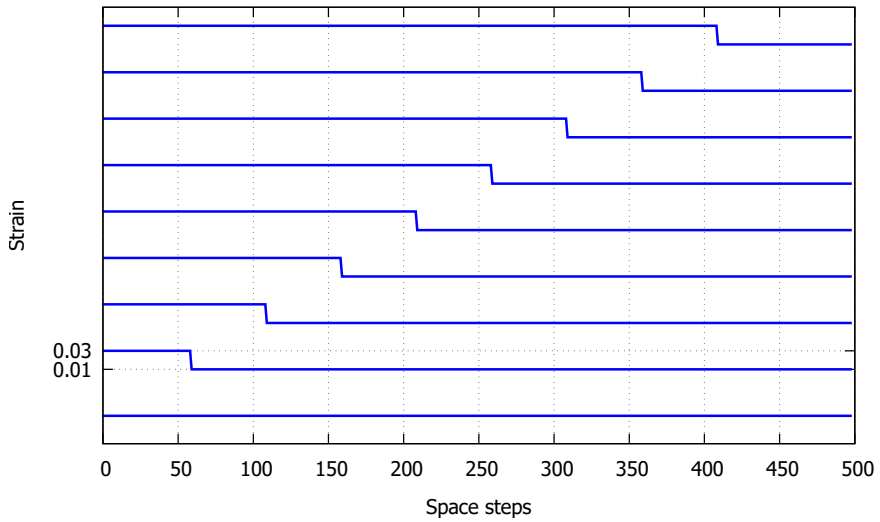

Figure 10. Distribution of shear strain along the bar plotted sequentially for every 50 time steps. The straight line at the bottom shows initial distribution of the shear strain.

initially in variant 2. The numerical features of the moving twin boundary treatment are responsible for the spikes in the stress distributions near the twin boundary.

The gradient of the internal variable retains its order parameter nature. Its variation in time repeats the motion of the twin boundary (Fig. 11).

The fast propagation of the twin boundary is confirmed by its position variation as shown in Fig. 12. After short time from the initiation of the motion, the velocity of the twin boundary becomes equal to the elastic speed.

As one can see, numerical simulations using the dual internal variable model demonstrate completely different behavior of twins in comparison with the diffusional growing in the single internal variable case. In the dual internal variable model, the twin boundary propagates along the bar with a high velocity. Such kind of the twin boundary dynamics can be corresponded to the twin tip propagation (Takeuchi 1966; Williams and Reid 1971; Kannan et al. 2018).

5 Conclusions

Classical continuum mechanics has no tools to describe equilibrium of twins, not to mention twin boundary motion. The experimental data of twin boundary propagation show a difference of 8 orders. To provide additional insight on the motion of twin

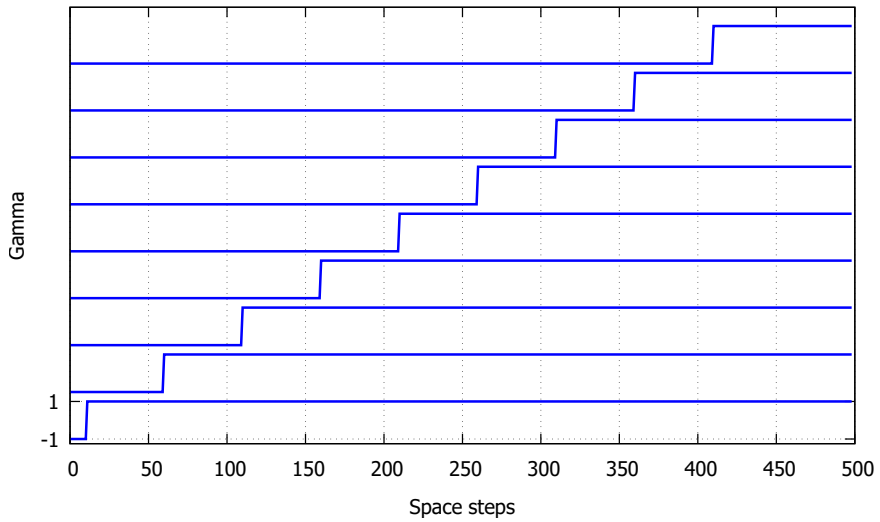

Figure 11. Distribution of gradient of internal variable along the bar plotted sequentially for every 50 time steps. The line at the bottom shows initial distribution of the gradient.

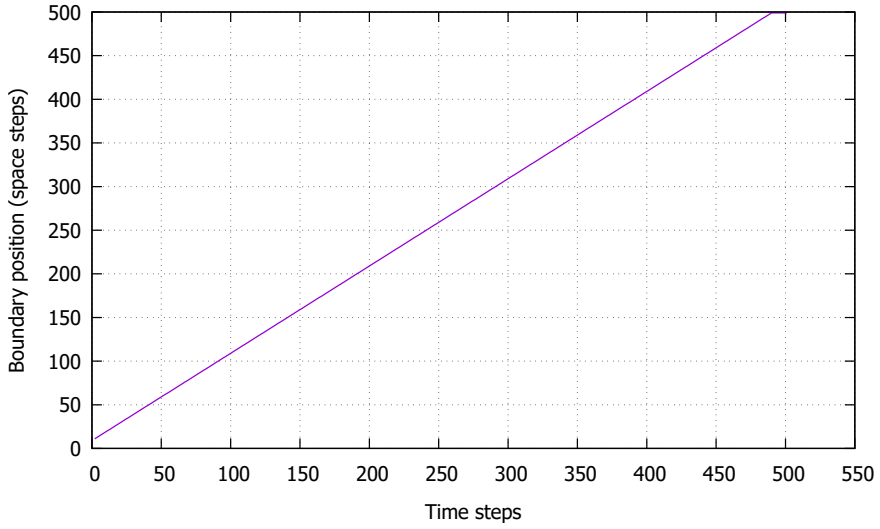

Figure 12. Variation in the twin boundary position in the case of dual internal variable model.

boundaries, the internal variable model is developed in the paper. The extension of the continuum description of twin boundary motion by internal variables allows for the

theoretical distinction between twin slow and fast dynamics. Internal variables serve as order parameters indicating the difference in twin variants. Equations of motion are coupled to evolution equations of internal variables. In the uniaxial case, these equations are solved numerically. A slow diffusional motion of a twin boundary is reproduced using a parabolic evolution equation in the case of a single internal variable. In contrast, the dual internal variable approach leads to a hyperbolic evolution equation for the evolution of the primary internal variable and provides fast dynamics of a twin boundary.

Acknowledgements

This research was supported by the Estonian Research Council under Research Project RPG1227, by the grant projects with No. GA22-00863K of the Czech Science Foundation (CSF) within institutional support RVO:61388998, and by the Mobility Czech-Estonia project EstAV-21-02. Valuable and helpful discussions with Prof. H. Seiner (IT ASCR Prague) are gratefully acknowledged.

Appendix. One-dimensional internal variables technique

Single internal variable

Here, basic notions of internal variable theory are reminded as they presented in (Berezovski 2018, e.g.).

In the linear elastic case, the one-dimensional motion of thermoelastic conductors of heat without body forces is governed by local balance laws for linear momentum and energy

$$(\rho v)_t - \sigma_x = 0, \tag{38}$$

$$\left(\frac{1}{2}\rho v^2 + \mathcal{E}\right)_t - (\sigma v - Q)_x = 0, \tag{39}$$

complemented by the second law of thermodynamics

$$S_t + \left(\frac{Q}{\theta} + K\right)_x \geq 0. \tag{40}$$

Here $\mathcal{E}$ is the internal energy per unit volume, S is the entropy per unit volume, θ is temperature, Q is the material heat flux, and the "extra entropy flux" K vanishes in most cases, but this is not a basic requirement.

In the single internal variable theory, the free energy W is specified as a sufficiently regular function of the strain, temperature, the internal variable, φ, and its space

gradient (Maugin and Muschik 1994). In the one-dimensional setting we have

$$W = \overline{W}(u_x, \theta, \varphi, \varphi_x). \tag{41}$$

The macroscopic stress σ, the entropy S, the internal stress η, and interactive internal force τ are determined by the equations of state

$$\sigma = \frac{\partial W}{\partial u_x}, \quad S = -\frac{\partial W}{\partial \theta}, \quad \tau := -\frac{\partial W}{\partial \varphi} \quad \eta := -\frac{\partial W}{\partial \varphi_x}. \tag{42}$$

In terms of the free energy per unit volume $W := E - S\theta$, the second law of thermodynamics (40) reads

$$-\left(W_t + S\theta_t\right) + \sigma\varepsilon_t + (\theta K)_x - \left(\frac{Q}{\theta} + K\right)\theta_x \geq 0. \tag{43}$$

Calculating the time rate of the free energy by chain rule

$$\begin{aligned} \frac{\partial W}{\partial t} &= \frac{\partial W}{\partial u_x}u_{xt} + \frac{\partial W}{\partial \theta}\theta_t + \frac{\partial W}{\partial \varphi}\varphi_t + \frac{\partial W}{\partial \varphi_x}\varphi_{xt} = \\ &= \sigma\varepsilon_t - S\theta_t - \tau\varphi_t - \eta\varphi_{xt}, \end{aligned} \tag{44}$$

we can represent dissipation inequality (43) as follows:

$$\tau\varphi_t + \eta\varphi_{xt} - \left(\frac{Q}{\theta} + K\right)\theta_x + (\theta K)_x \geq 0. \tag{45}$$

To rearrange the dissipation inequality, we add and subtract the same term $\eta_x\varphi_t$

$$\tau\varphi_t + \eta\varphi_{xt} - \eta_x\varphi_t + \eta_x\varphi_t - \left(\frac{Q}{\theta} + K\right)\theta_x + (\theta K)_x \geq 0, \tag{46}$$

resulting in another form of the dissipation inequality

$$(\tau - \eta_x)\varphi_t - \left(\frac{Q}{\theta} + K\right)\theta_x + (\eta\varphi_t + \theta K)_x \geq 0. \tag{47}$$

As one can see, the first two terms in the left hand side of Eq. (47) are products of thermodynamic fluxes and forces, whereas the last term represents the divergence of a certain quantity. This divergence term can be eliminated by choosing of the extra entropy flux as follows:

$$K = -\theta^{-1}\eta\varphi_t. \tag{48}$$

This method of the elimination of divergences has its roots in the classical irreversible thermodynamics (De Groot and Mazur 1962) and has been formulated explicitly in case of internal variables by Maugin (1990). Then dissipation inequality Eq. (47) reduces to

$$(\tau - \eta_x)\varphi_t - \frac{Q + \eta\varphi_t}{\theta}\theta_x \geq 0. \tag{49}$$

It is remarkable that in the isothermal case ($\theta_x = 0$) the dissipation is determined in terms of the internal variable only.

Evolution equation for a single internal variable

In the *isothermal* case the dissipation inequality (49) is even more simple

$$(\tau - \eta_x)\varphi_t \geq 0. \tag{50}$$

The linear solution of this inequality represents the evolution equation for the internal variable

$$\varphi_t = k(\tau - \eta_x), \quad k \geq 0, \tag{51}$$

since dissipation inequality (50) is satisfied automatically in this case

$$\Phi = k\varphi_t^2 \geq 0, \quad \text{if} \quad k \geq 0. \tag{52}$$

The fully non-dissipative case corresponds to $k = 0$.

To see how obtained evolution equation for the internal variable (51) looks like, we specify the free energy dependence in the isothermal case to a quadratic one

$$W = \frac{G}{2}u_x^2 + \frac{1}{2}A\varphi_x u_x + \frac{1}{2}B\varphi^2 + \frac{1}{2}C\varphi_x^2, \tag{53}$$

where G is the Young modulus and A, B, and C are material parameters. It follows from equations of state that

$$\tau = -\frac{\partial W}{\partial \varphi} = -B\varphi, \quad \eta = -\frac{\partial W}{\partial \varphi_x} = -\frac{1}{2}Au_x - C\varphi_x, \tag{54}$$

and evolution equation (51) is an equation of reaction-diffusion type

$$\frac{1}{k}\varphi_t = C\varphi_{xx} + \frac{1}{2}Au_{xx} - B\varphi. \tag{55}$$

It is clear that Eq. (55) is the Ginzburg-Landau-type equation. The macrostress is calculated as follows:

$$\sigma = \frac{\partial W}{\partial u_x} = G u_x + \frac{1}{2} A \varphi_x, \tag{56}$$

and the balance of linear momentum reads

$$\rho v_t = G \varepsilon_x + \frac{1}{2} A \varphi_{xx}. \tag{57}$$

Equations (55) and (57) are the governing equations in the single internal variable model. To be independent of the choice of a material, we represent governing equations in the dimensionless form.

Dimensionless variables

Let t_0 is a characteristic time of a process and L is its characteristic length. Dimensionless variables are introduced as follows:

$$T = \frac{t}{t_0}, \quad X = \frac{x}{L}, \quad U = \frac{u}{L}, \quad \Phi = \frac{\varphi}{L}. \tag{58}$$

Substitution of definitions (58) into Eqs. (55) and (57) provides

$$U_{TT} = \frac{t_0^2}{\rho L^2} \left(G U_{XX} + \frac{1}{2} A \Phi_{XX} \right), \tag{59}$$

$$\Phi_T = \frac{A k t_0}{L^2} \left(\frac{C}{A} \Phi_{XX} + \frac{1}{2} U_{XX} - \frac{B}{A} L^2 \Phi \right). \tag{60}$$

The choice of characteristic value t_0 is dictated by keeping the same order of magnitude for terms in the left-hand side and right-hand side of Eq. (60)

$$t_0 = \frac{L^2}{Ak}. \tag{61}$$

Such a choice results in the dimensionless balance of linear momentum

$$U_{TT} = \frac{L^2}{\rho A^2 k^2} \left(G U_{XX} + \frac{1}{2} A \Phi_{XX} \right). \tag{62}$$

To simplify the matter, it is convenient to set $k = L\sqrt{G/\rho}/A$. Then we arrive at

$$U_{TT} = U_{XX} + \frac{1}{2} \frac{A}{G} \Phi_{XX}. \tag{63}$$

Correspondingly, the dimensionless evolution equation for the internal variable obtains the form

$$\Phi_T = \frac{C}{A}\Phi_{XX} + \frac{1}{2}U_{XX} - \frac{B}{A}L^2\Phi. \tag{64}$$

The governing parameters of the problem are the dimensionless coefficients A/G, BL^2/A and C/A. The characteristic time of the process is

$$t_0 = \frac{L}{\sqrt{G/\rho}}. \tag{65}$$

For $B \equiv 0$ we denote

$$\bar{v} = U_T, \quad \bar{\varepsilon} = U_X, \quad \bar{\gamma} = \Phi_x, \tag{66}$$

and rewrite the governing equations as follows:

$$\bar{v}_T = \bar{\varepsilon}_X + \frac{1}{2}\frac{A}{G}\bar{\gamma}_X, \quad \bar{\gamma}_T = \frac{C}{A}\bar{\gamma}_{XX} + \frac{1}{2}\bar{\varepsilon}_{XX}. \tag{67}$$

Just these equations are solved numerically in Section 5. Thus, we have dimensionless governing parameters $A/G = \varepsilon^{tr}$ and $C/G = (\varepsilon^{tr})^2/4$ which depend on the transformation strain.

Dual internal variables

The complete theory of dual internal variables is presented in (Berezovski and Ván 2017, e.g.). Here we use a reduced version of the theory assuming that the free energy density depends on internal variables φ and ψ by virtue of a quadratic function

$$W = \frac{G}{2}u_x^2 + \frac{1}{2}A\varphi_x u_x - \frac{1}{2}C\varphi_x^2 - \frac{1}{2}D\psi^2, \tag{68}$$

where material parameters A, C, and D are constant. In this version, the free energy does not depend on the internal variable φ explicitly and on the gradient of the internal variable ψ. Negative signs for coefficients C and D are applied in the correspondence to (Berezovski 2016).

By definition, the Cauchy stress is calculated as follows:

$$\sigma = \frac{\partial W}{\partial u_x} = Gu_x + \frac{1}{2}A\varphi_x. \tag{69}$$

Similarly, the internal stresses are defined by

$$\eta = -\frac{\partial W}{\partial \varphi_x} = -\frac{1}{2}Au_x + C\varphi_x, \tag{70}$$

$$\zeta = -\frac{\partial W}{\partial \psi_x} = 0. \tag{71}$$

Affinities with respect to the dual internal variables are, respectively,

$$\tau = -\frac{\partial W}{\partial \varphi} = 0, \quad \xi = -\frac{\partial W}{\partial \psi} = D\psi. \tag{72}$$

Proceeding similarly to the single internal variable case, we can represent the dissipation inequality in the isothermal case in the form (Berezovski and Ván 2017; Berezovski 2018)

$$(\tau - \eta_x)\varphi_t + (\xi - \zeta_x)\psi_t \geq 0. \tag{73}$$

It is clear that the choice

$$\varphi_t = (\xi - \zeta_x), \qquad \psi_t = -(\tau - \eta_x), \tag{74}$$

leads to zero dissipation.

Due to Eqs. (71) and (72), evolution equation for the internal variable φ $(74)_1$ is reduced to

$$\varphi_t = D\psi. \tag{75}$$

Time derivative of Eq. (75) and evolution equation for the dual internal variable $(74)_2$ determine the hyperbolic evolution equation for the internal variable φ

$$\frac{1}{D}\varphi_{tt} = C\varphi_{xx} - \frac{1}{2}A\varepsilon_x. \tag{76}$$

It is convenient to introduce the time rate of the internal variable φ and its gradient

$$\varphi_t = w, \quad \varphi_x = \gamma. \tag{77}$$

In terms of the time rate, w and the internal strain gradient, γ we have the system of first-order equations

$$Iw_t = C\gamma_x - \frac{1}{2}A\varepsilon_x, \tag{78}$$

$$\gamma_t = w_x, \tag{79}$$

with $I = 1/D$. The balance of linear momentum in the form

$$\rho v_t = G\varepsilon_x + \frac{1}{2}A\gamma_x, \tag{80}$$

is complemented by kinematic compatibility condition

$$\varepsilon_t = v_x, \tag{81}$$

Equations (76) – (81) represent the dual internal variable model in one dimensional setting.

Dimensionless variables

To determine governing parameters of the problem, we introduce dimensionless variables

$$U = \frac{u}{L}, \quad X = \frac{x}{L}, \quad T = \frac{t}{t_0}, \quad \Phi = \frac{\varphi}{L}. \tag{82}$$

In terms of dimensionless variables, equations (76) and (80) read

$$I\Phi_{TT} = \frac{t_0^2}{L^2}\left(C\Phi_{XX} - \frac{1}{2}AU_{XX}\right), \tag{83}$$

$$U_{TT} = \frac{Gt_0^2}{\rho L^2}\left(U_{XX} + \frac{1}{2}A\Psi_{XX}\right). \tag{84}$$

The choice of the characteristic time is dictated by the same order in value of the both parts of Eq. (84)

$$t_0 = \frac{L}{\sqrt{G/\rho}}. \tag{85}$$

Then Eq. (83) reduces to

$$\frac{I}{\rho}\Phi_{TT} = \frac{C}{G}\Phi_{XX} - \frac{A}{G}U_{XX}, \tag{86}$$

and Eq. (84) remains the same as Eq. (63)

$$U_{TT} = U_{XX} + \frac{1}{2}\frac{A}{G}\Phi_{XX}. \tag{87}$$

References

Abeyaratne R and Knowles JK (1990) On the driving traction acting on a surface of strain discontinuity in a continuum. *Journal of the Mechanics and Physics of Solids* 38(3): 345–360. DOI:10.1016/0022-5096(90)90003-M.

Abeyaratne R and Knowles JK (2006) *Evolution of Phase Transitions: A Continuum Theory*. Cambridge University Press.

Amirian B, Jafarzadeh H, Abali BE, Reali A and Hogan JD (2022) Phase-field approach to evolution and interaction of twins in single crystal magnesium. *Computational Mechanics* 70(4): 803–818. DOI:10.1007/s00466-022-02209-3.

Auricchio F and Lubliner J (1997) A uniaxial model for shape-memory alloys. *International Journal of Solids and Structures* 34(27): 3601–3618. DOI:10.1016/S0020-7683(96)00232-6.

Berezovski A (2016) On the Mindlin microelasticity in one dimension. *Mechanics Research Communications* 77: 60–64. DOI:10.1016/j.mechrescom.2016.09.005.

Berezovski A (2018) Internal variables associated with microstructures in solids. *Mechanics Research Communications* 93: 30–34. DOI:10.1016/j.mechrescom.2017.07.011.

Berezovski A (2023) Constitutive modeling with single and dual internal variables. *Entropy* 25(5): 721. DOI:10.3390/e25050721.

Berezovski A, Engelbrecht J and Maugin GA (2008) *Numerical Simulation of Waves and Fronts in Inhomogeneous Solids*. World Scientific.

Berezovski A and Ván P (2017) *Internal Variables in Thermoelasticity*. Springer.

Bhattacharya K (2003) *Microstructure of Martensite: why it forms and how it gives rise to the shape-memory effect*. Oxford University Press.

Bowden F and Cooper R (1962) Velocity of twin propagation in crystals. *Nature* 195(4846): 1091–1092. DOI:10.1038/1951091a0.

Brinson L and Huang M (1996) Simplifications and comparisons of shape memory alloy constitutive models. *Journal of Intelligent Material Systems and Structures* 7(1): 108–114. DOI:10.1177/1045389X9600700112.

Brinson LC (1993) One-dimensional constitutive behavior of shape memory alloys: thermomechanical derivation with non-constant material functions and redefined martensite internal variable. *Journal of Intelligent Material Systems and Structures* 4(2): 229–242. DOI:10.1177/1045389X9300400213.

Danino B, Gur-Arieh G, Shilo D and Mordehai D (2019) Relations between material properties and barriers for twin boundary motion in ferroic materials. *Acta Materialia* 180: 24–34. DOI:10.1016/j.actamat.2019.08.016.

De Groot SR and Mazur P (1962) *Non-equilibrium Thermodynamics*. North Holland.

Duparc OH (2017) A review of some elements for the history of mechanical twinning centred on its German origins until Otto Mügge's K 1 and K 2 invariant plane notation. *Journal of Materials Science* 52(8): 4182–4196. DOI:10.1007/s10853-016-0513-4.

Falk F (1980) Model free energy, mechanics, and thermodynamics of shape memory alloys. *Acta Metallurgica* 28(12): 1773–1780. DOI:doi:10.1016/0001-6160(80)90030-9.

Faran E and Shilo D (2010) Twin motion faster than the speed of sound. *Physical Review Letters* 104(15): 155501. DOI:10.1103/PhysRevLett.104.155501.

Faran E and Shilo D (2011) The kinetic relation for twin wall motion in NiMnGa. *Journal of the Mechanics and Physics of Solids* 59(5): 975–987. DOI:10.1016/j.jmps.2011.02.009.

Faran E and Shilo D (2014) Dynamics of twin boundaries in ferromagnetic shape memory alloys. *Materials Science and Technology* 30(13): 1545–1558. DOI: 10.1179/1743284714y.0000000570.

Faran E and Shilo D (2016) Ferromagnetic shape memory alloys—challenges, applications, and experimental characterization. *Experimental Techniques* 40: 1005–1031. DOI: 10.1007/s40799-016-0098-5.

Grilli N, Cocks AC and Tarleton E (2020) A phase field model for the growth and characteristic thickness of deformation-induced twins. *Journal of the Mechanics and Physics of Solids* 143: 104061. DOI:10.1016/j.jmps.2020.104061.

Gu Y, Chen LQ, Heo TW, Sandoval L and Belak J (2013) Phase field model of deformation twinning in tantalum: Parameterization via molecular dynamics. *Scripta Materialia* 68(7): 451–454. DOI:10.1016/j.scriptamat.2012.11.022.

Hu S, Henager CH and Chen L (2010) Simulations of stress-induced twinning and de-twinning: A phase field model. *Acta Materialia* 58(19): 6554–6564. DOI: 10.1016/j.actamat.2010.08.020.

Kannan V, Hazeli K and Ramesh K (2018) The mechanics of dynamic twinning in single crystal magnesium. *Journal of the Mechanics and Physics of Solids* 120: 154–178. DOI: 10.1016/j.jmps.2018.03.010.

Khandelwal A and Buravalla V (2009) Models for shape memory alloy behavior: an overview of modeling approaches. *The International Journal of Structural Changes in Solids* 1(1): 111–148.

Levitas VI, Roy AM and Preston DL (2013) Multiple twinning and variant-variant transformations in martensite: Phase-field approach. *Physical Review B* 88(5). DOI: 10.1103/physrevb.88.054113.

Liu C, Shanthraj P, Diehl M, Roters F, Dong S, Dong J, Ding W and Raabe D (2018) An integrated crystal plasticity–phase field model for spatially resolved twin nucleation,

propagation, and growth in hexagonal materials. *International Journal of Plasticity* 106: 203–227. DOI:10.1016/j.ijplas.2018.03.009.

Mahajan S and Williams D (1973) Deformation twinning in metals and alloys. *International Metallurgical Reviews* 18(2): 43–61. DOI:10.1179/imtlr.1973.18.2.43.

Maugin GA (1990) Internal variables and dissipative structures. *Journal of Non-Equilibrium Thermodynamics* 15(2): 173–192. DOI:10.1515/jnet.1990.15.2.173.

Maugin GA and Muschik W (1994) Thermodynamics with internal variables. Part I. General concepts. *Journal of Non Equilibrium Thermodynamics* 19: 217–249. DOI: 10.1515/jnet.1994.19.3.217.

Mirkhani H and Joshi SP (2014) Mechanism-based crystal plasticity modeling of twin boundary migration in nanotwinned face-centered-cubic metals. *Journal of the Mechanics and Physics of Solids* 68: 107–133. DOI:10.1016/j.jmps.2014.03.006.

Mirzaeifar R, DesRoches R and Yavari A (2011) Analysis of the rate-dependent coupled thermo-mechanical response of shape memory alloy bars and wires in tension. *Continuum Mechanics and Thermodynamics* 23(4): 363–385. DOI:10.1007/s00161-011-0187-8.

Mizrahi A, Shilo D and Faran E (2020) Variability of twin boundary velocities in 10M Ni–Mn–Ga measured under μs-scale force pulses. *Shape Memory and Superelasticity* : 1–9DOI: 10.1007/s40830-020-00264-4.

Otsuka K and Wayman CM (1999) *Shape Memory Materials*. Cambridge University Press.

Paiva A and Savi MA (2006) An overview of constitutive models for shape memory alloys. *Mathematical Problems in Engineering* 2006. DOI:10.1155/MPE/2006/56876.

Rasmussen K, Lookman T, Saxena A, Bishop A, Albers R and Shenoy S (2001) Three-dimensional elastic compatibility and varieties of twins in martensites. *Physical Review Letters* 87(5): 055704. DOI:10.1103/PhysRevLett.87.055704.

Reed-Hill RE, Abbaschian R and Abbaschian L (1973) *Physical Metallurgy Principles*. Van Nostrand, New York.

Rezaee-Hajidehi M, Sadowski P and Stupkiewicz S (2022) Deformation twinning as a displacive transformation: Finite-strain phase-field model of coupled twinning and crystal plasticity. *Journal of the Mechanics and Physics of Solids* 163: 104855. DOI: 10.1016/j.jmps.2022.104855.

Rosakis P and Tsai H (1995) Dynamic twinning processes in crystals. *International Journal of Solids and Structures* 32(17-18): 2711–2723. DOI:10.1016/0020-7683(94)00293-6.

Sadjadpour A and Bhattacharya K (2007) A micromechanics-inspired constitutive model for shape-memory alloys. *Smart Materials and Structures* 16(5): 1751. DOI:10.1088/0964-1726/16/5/030.

Saren A, Nicholls T, Tellinen J and Ullakko K (2016) Direct observation of fast-moving twin boundaries in magnetic shape memory alloy Ni–Mn–Ga 5 M martensite. *Scripta Materialia* 123: 9–12. DOI:10.1016/j.scriptamat.2016.04.004.

Seiner H (2015) Highly mobile interfaces in shape memory alloys. *MATEC Web of Conferences* 33: 01002. DOI:10.1051/matecconf/20153301002.

Seiner H, Zelený M, Sedlák P, Straka L and Heczko O (2022) Experimental observations versus first-principles calculations for ni–mn–ga ferromagnetic shape memory alloys: A review. *Physica Status Solidi (RRL) – Rapid Research Letters* 16(6). DOI:10.1002/pssr.202100632.

Shchyglo O, Salman U and Finel A (2012) Martensitic phase transformations in Ni–Ti-based shape memory alloys: The Landau theory. *Acta Materialia* 60(19): 6784–6792. DOI: 10.1016/j.actamat.2012.08.056.

Shilo D, Faran E, Karki B and Müllner P (2021) Twin boundary structure and mobility. *Acta Materialia* 220: 117316. DOI:10.1016/j.actamat.2021.117316.

Smith AR, Tellinen J and Ullakko K (2014) Rapid actuation and response of Ni–Mn–Ga to magnetic-field-induced stress. *Acta Materialia* 80: 373–379. DOI: 10.1016/j.actamat.2014.06.054.

Song Z (2020) Analytical study on phase transition of shape memory alloy wire under uniaxial tension. *International Journal of Engineering Science* 152: 103295. DOI: 10.1016/j.ijengsci.2020.103295.

Takeuchi T (1966) Dynamic propagation of deformation twins in iron single crystals. *Journal of the Physical Society of Japan* 21(12): 2616–2622. DOI:10.1143/JPSJ.21.2616.

Tanaka K, Kobayashi S and Sato Y (1986) Thermomechanics of transformation pseudoelasticity and shape memory effect in alloys. *International Journal of Plasticity* 2(1): 59–72. DOI: 10.1016/0749-6419(86)90016-1.

Tanaka K and Nagaki S (1982) A thermomechanical description of materials with internal variables in the process of phase transitions. *Ingenieur-Archiv* 51(5): 287–299. DOI: 10.1007/BF00536655.

Ván P, Berezovski A and Engelbrecht J (2008) Internal variables and dynamic degrees of freedom. *Journal of Non-Equilibrium Thermodynamics* 33(3): 235–254. DOI: 10.1515/jnetdy.2008.010.

Williams D and Reid G (1971) A dynamic study of twin-induced brittle fracture. *Acta Metallurgica* 19(9): 931–937. DOI:10.1016/0001-6160(71)90086-1.

Zhao F, Wang L, Fan D, Bie B, Zhou X, Suo T, Li Y, Chen M, Liu C, Qi M et al. (2016) Macrodeformation twins in single-crystal aluminum. *Physical Review Letters* 116(7): 075501. DOI:10.1103/PhysRevLett.116.075501.

Zoubková K, Seiner H, Sedlák P, Villa E, Tahara M, Hosoda H and Chernenko V (2022) Nonlinear elastic behavior of Ni-Fe-Ga (Co) shape memory alloy and Landau-energy landscape reconstruction. *Acta Materialia* 224: 117530. DOI:10.1016/j.actamat.2021.117530.